

IFSCC 2025 full paper (IFSCC2025-647)

## ***“Development of an Advanced System for Estimating the Number of Overlapping Hair Cuticles Through the Analysis of Hair Surface Image Data Utilizing a Newly Developed AI Model”***

**Kumiko Seki<sup>1,\*</sup>, Masataka Kubouchi<sup>2</sup>, Shuji Sugie<sup>1</sup>, Takuma Nishimoto<sup>2</sup>,  
Ippei Horibe<sup>1</sup>, Yasunari Matsumoto<sup>2</sup>, Ryoji Ishihara<sup>1</sup>**

<sup>1</sup> Research & Development Division, NAKANO SEIYAKU CO., LTD., Kyoto, Japan

<sup>2</sup> KNiT Inc., Osaka, Japan

### **Abstract**

The cuticle on the hair surface forms a layered structure, with Japanese individuals typically exhibiting 6 to 10 overlapping layers. The number of these layers significantly influences hair properties. As these layers are damaged and gradually peel off due to external stimuli, the remaining count serves as an important indicator of hair health. This study aims to develop a novel method for objectively and efficiently estimating the cuticle layer counts from hair surface images by constructing an artificial intelligence (AI) model, which is trained on various features extracted from both hair surface and cross-sectional images. Hair surface images with identifiable cuticle structures were captured using a digital microscope from arbitrary sections of hair samples ( $N = 243$ ) collected from 56 Japanese participants (aged 14–74, including both males and females). The cuticle layer counts in the imaged regions were manually measured, and their correlation with various cuticle shape features extracted from the images were analyzed. Features that showed strong correlations were selected to construct an AI model capable of estimating the cuticle layer counts. We identified significant correlations between the manually measured cuticle layer counts and specific features derived from the hair surface images. Machine learning results revealed that correlated features were the mean and standard deviation of the diagonal width, the shorter side of the bounding rectangle, area, tilt angle and deviation from mode angle. Using these correlated features, we constructed an AI model capable of estimating the cuticle layer counts. The AI's estimates closely matched the measured values, validating the effectiveness of the selected features and the model. The cuticle layer counts on the hair surface varies depending on the individual, age, and even the specific region observed within the same individual. This count is an important factor in determining hair characteristics and influences decisions made by professionals, such as hairstylists, when selecting beauty treatments to enhance aesthetic value. Therefore, the AI model developed in this study estimates the cuticle layer counts from hair surface images, aiding in the delivery of optimized aesthetic value tailored to individual characteristics. Additionally, through detailed data analysis by gender and age, it contributes to future predictions, with the potential to create novel aesthetic values throughout life.

## 1. Introduction

In hair salons, hair condition of customers is typically assessed subjectively based on treatment history, hairstylists' sensory evaluations, and customer self-reports, with treatments then being tailored accordingly. For example, during perming and hair coloring procedures, hairstylists evaluate the hair condition, including the degree of damage and other hair properties, to select appropriate chemical agents that will achieve the desired hair wave or color. Inaccurate selection of these agents can lead to insufficient or excessive penetration, resulting in unsatisfactory outcomes. Similarly, the selection of hair care products is crucial, as inaccurate choices may fail to improve the hair's texture.

Scanning electron microscopy (SEM) is commonly used for assessing hair damage, where images of the hair surface are compared to a reference scale of damage grades [1-3]. This method is relatively simple, but it is limited to surface evaluation, and variations in the assessment can occur. In contrast, methods that directly observe the overlapping cuticle layer counts from cross-sectional images of the hair or algorithms developed using atomic force microscopy (AFM) have been reported [4][5]. However, these methods require destructive sample preparation or specialized equipment, making them impractical for use in hair salons.

The cuticle on the hair surface has a layered structure. Typically, each cuticle layer is about 0.5 µm thick and 45–60 µm in length, arranged with an approximate 5° angle relative to the hair shaft. Approximately 5 µm of the total length is exposed on the surface [6]. In Japanese hair, the overlapping cuticle layer counts is typically between 6 and 10, and this number significantly impacts the hair's properties. The cuticle is susceptible to damage from external stimuli such as heat, friction, and chemical treatments, leading to missing layers and a decrease in the number of overlaps [7]. Traditional methods have made it difficult to accurately capture these changes, creating a need for a more precise approach to monitor the changes in the overlapping cuticle layer counts [2][8]. This study aims to develop a new artificial intelligence (AI) model that objectively and efficiently estimates the overlapping cuticle layer counts from hair surface images, thereby supporting the optimal provision of cosmetic hair services tailored to hair characteristics.

## 2. Materials and Methods

### 2.1. Estimating the Overlapping Cuticle Layer Counts

To estimate the overlapping cuticle layer counts from hair surface images, the process involves the following steps: image acquisition, cuticle shape recognition using a region recognition model, feature extraction, and estimation of the overlapping cuticle layer counts using an estimation model. The overall workflow is illustrated in Figure 1.

### 2.2. Image Acquisition Step

#### 2.2.1. Hair Samples

Hair samples were collected from 56 Japanese participants (24 males and 32 females) ranging in age from 14 to 74 years. Samples were taken from three regions of the scalp: the crown, above the ear, and the midpoint between these two areas. These samples were subsequently used for the analysis. All human-related experiments were conducted in accordance with the principles of the Declaration of Helsinki. Full disclosure of all procedures was provided, and written informed consent was obtained from all participants in advance.

#### 2.2.2. Hair Surface Image Data

A total of 243 hair strands were sampled. Surface images were acquired approximately 1 cm from both the proximal (root) and distal (tip) ends using a digital microscope with 1000×

magnification and a resolution of  $2880 \times 2160$  pixels. To capture detailed surface morphology, both ring and coaxial illumination were utilized simultaneously.

### 2.2.3. Measurement of the Overlapping Cuticle Layer counts

To determine the overlapping cuticle layer counts, the hair strands were diagonally sectioned to obtain inclined cross-sectional surfaces. Images of these sections were captured using the same digital microscope under coaxial oblique illumination at  $2000\times$  magnification. The overlapping cuticle layer counts were manually counted from these inclined cross-sectional images.

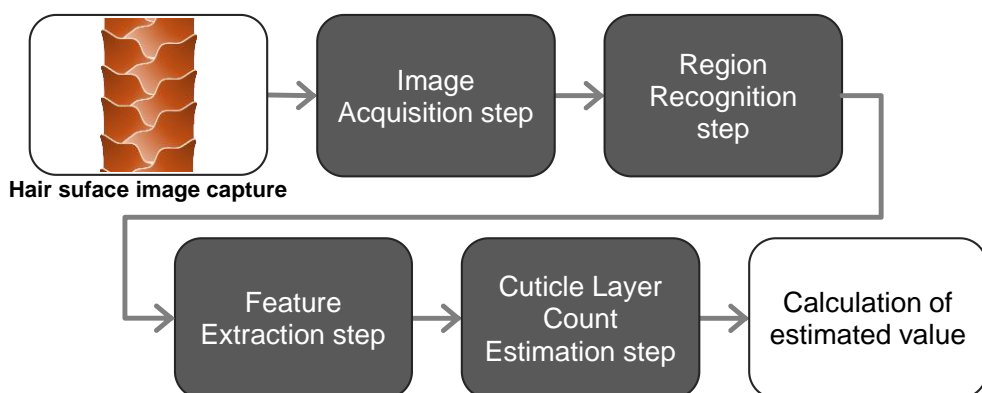


**Figure 1.** Workflow for Estimating the Overlapping Cuticle Layer Counts from Hair Surface Images

The process begins with capturing the surface image of a hair strand, followed by acquisition of image data. Specific regions on the hair surface are identified, and relevant features related to texture and structure are extracted. These features are then used to estimate the overlapping cuticle layer counts. Finally, the predicted value is calculated based on the extracted features.

## 2.3. Region Recognition Step

### 2.3.1. Image Analysis Algorithm

AI-based image analysis methods include anomaly detection, object detection, and segmentation. A common and essential component across all these tasks is a neural network structure for extracting image features, known as a convolutional neural network (CNN). This feature-extraction component, referred to as the "backbone," typically includes architectures such as ResNet [9], Inception [10], and Vision Transformer (ViT) [11]. In this study, ResNet50 was employed as backbones to extract image features. Since the default pretrained backbones did not yield sufficient accuracy, fine-tuning was performed to develop the AI models. Furthermore, as numerical analysis of the images was required, segmentation techniques were utilized. Among the available segmentation approaches—semantic segmentation, instance segmentation, and panoptic segmentation, instance segmentation was selected, as it enables individual objects to be distinguished separately.

### 2.3.2. Ground Truth Data Preparation (Region Recognition Model)

To identify cuticle regions on the hair surface, techniques such as edge detection were employed to delineate boundaries based on the step-like changes caused by the overlapping structure of individual cuticles. Each cuticle's outline was defined by enclosing these boundaries, allowing for clear segmentation of cuticle regions. Subsequently, the coordinates of each segmented cuticle region were determined, and annotation tools or segmentation software were used to label these regions within the image data. A large set of paired data—comprising surface images of hair and the corresponding labeled cuticle regions—was prepared and used as the ground truth dataset for training the region recognition model.

## 2.4. Feature Extraction Step

Using the annotated dataset described in Section 2.3.2. an image analysis AI model was developed to recognize cuticles on the hair surface and extract relevant features. Representative extracted features included: the number of detected cuticles, area, maximum length, diagonal length, shorter and longer side of bounding rectangle, deviation from mode angle, aspect ratio, mean pixel intensity, and roundness. These features were then used in a machine learning-based analysis to investigate their relationship with the overlapping cuticle layer counts.

## 2.5. Cuticle Layer Count Estimation Step

### 2.5.1. Machine Learning Method

Various machine learning algorithms can be applied to regression and classification tasks, including neural networks, linear regression, support vector machines, random forests, and deep learning. In this study, we employed a random forest algorithm, which is well-suited for small-scale datasets and capable of both classification and regression. In this study, the features consisted of 23-dimensional data obtained from image analysis, which included some features that were not important for the prediction. Typically, the selection of effective features from a large set of features is a subjective process reliant on the expertise and intuition of the researcher. In this study, we first extracted features that showed statistically significant correlations with the overlapping cuticle layer counts. These selected features were then used to construct a random forest model to estimate the cuticle layer counts. The dataset was split into training and testing subsets at a ratio of 8:2. After training the model using the training data, we evaluated its prediction accuracy using the test data.

### 2.5.2. Ground Truth Data Preparation (Cuticle Layer Count Estimation Model)

Using the annotated dataset developed for the region recognition model, we calculated feature values for each cuticle region delineated by boundary lines in the images. These features were expressed as quantitative numerical values and computed using commonly available programming tools, such as OpenCV. The extracted features served as features, and the manually measured cuticle layer counts described in Section 2.2.3. were used as the target variable. A large number of data pairs were thus constructed and used as the ground truth dataset for training the estimation model. To evaluate the average predictive performance of the developed model, we applied it to the test dataset and compared the estimated cuticle layer counts with the corresponding measured values.

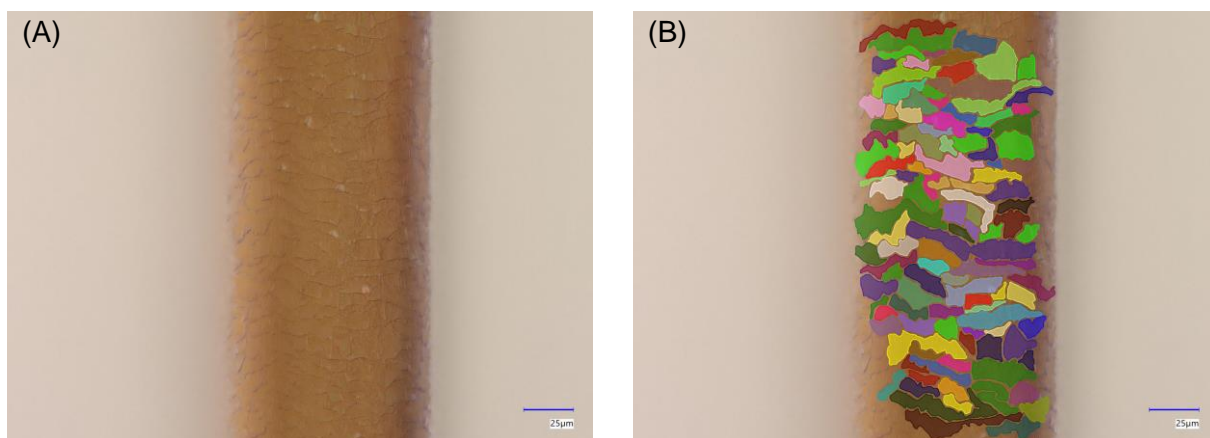


**Figure 2.** Hair surface image and the result of cuticle region recognition

(A) Captured image of the hair surface, (B) Image showing the recognized cuticle fragment regions by the segmentation model.

### 3. Results

#### 3.1. Relationship Between Cuticle Morphology and Overlapping Layer Counts

The analysis of the hair surface images confirmed that the AI model was able to effectively identify cuticle regions, as evident from the captured hair surface image and the corresponding recognized cuticle areas (Figure 2). The feature extraction process based on hair surface images yielded measurements including the maximum length, diagonal length, aspect ratio, tilt angle, area, and color of each cuticle, hair width (Table 1). These features were subjected to correlation analysis against the overlapping cuticle layer counts.

#### 3.2. Feature Selection and Construction of the Cuticle Layer Count Estimation Model

We examined the correlation between various features obtained from hair surface images and the overlapping cuticle layer counts (Table 2). The p-values were calculated using permutation tests, which assess the statistical significance by comparing the observed correlation coefficient with a distribution obtained by randomly rearranging the data. This allows for significance testing without assuming a normal distribution. In the table, the p-value represents the probability that the correlation coefficient of the randomly shuffled sample data exceeds the original correlation coefficient. The permutation process was performed 1,000 times, and a significance level of 5% was used, with p-values below 0.05 being considered significant. Features deemed significant were grouped based on the absolute value of their correlation coefficients. The mean and standard deviation of each cuticle's diagonal length, shorter side of bounding rectangle, deviation from mode angle, area, and tilt angle showed a strong correlation with the measured overlapping cuticle layer counts. The results of the machine learning analysis suggest that greater cuticle alignment, a higher number of detectable cuticle regions, and shorter lengths of the minor axis of the cuticle's bounding rectangle were associated with more overlapping cuticle layers, reflecting better cuticle integrity.

Random forest models were constructed based on these correlation groups to predict the overlapping cuticle layer counts. The performance of each model was compared with a simple baseline model that outputs the mean value, with a baseline RMSE of 1.2766. Models with lower RMSE than the baseline were considered significant. RMSE indicates the magnitude of

**Table1.** Summary of Extracted Features and Categories

Category	Feature (Mean)	Feature (SD)
<b>Shape-related features</b>	Aspect ratio	SD of aspect ratio
	Tilt angle (°)	SD of tilt angle (°)
	Roundness	SD of roundness
	Equivalent diameter ( $\mu\text{m}$ )	SD of equivalent diameter ( $\mu\text{m}$ )
	Shorter side of bounding rectangle ( $\mu\text{m}$ )	SD of shorter side of bounding rectangle ( $\mu\text{m}$ )
	Longer side of bounding rectangle ( $\mu\text{m}$ )	SD of longer side of bounding rectangle ( $\mu\text{m}$ )
	Diagonal length ( $\mu\text{m}$ )	SD of diagonal length ( $\mu\text{m}$ )
	Deviation from mode angle (°)	SD of deviation from mode angle (°)
	Maximum absolute length ( $\mu\text{m}$ )	SD of maximum absolute length ( $\mu\text{m}$ )
<b>Count-related features</b>	Number of detected cuticles	SD of number of detected cuticles
<b>Area/size features</b>	Area ( $\mu\text{m}^2$ )	SD of area ( $\mu\text{m}^2$ )
	Hair width ( $\mu\text{m}$ )	SD of hair width ( $\mu\text{m}$ )
<b>Color features</b>	Mean pixel value – Grayscale	SD of pixel value – Grayscale
	Mean pixel value – Hue (H)	SD of pixel value – Hue
	Mean pixel value – Lightness ( $L^*$ )	SD of pixel value – Lightness
	Mean pixel value – Saturation (S)	SD of pixel value – Saturation
	Mean pixel value – Value (V)	SD of pixel value – Value
	Mean pixel value – $a^*$	SD of pixel value – $a^*$
	Mean pixel value – $b^*$	SD of pixel value – $b^*$

Note:

- SD: Standard Deviation;  $\mu\text{m}$  : micrometer;  $L^*$ ,  $a^*$ ,  $b^*$  : color components in CIELAB color space; H, S, V : hue, saturation, value; All features are computed per image and include both mean and standard deviation.

**Table2.** Correlation Analysis Between Cuticle Morphological Features and Overlapping Layer Counts

No.	Feature	Pearson's r	r	p-value	Correlation Group
1	Mean of diagonal length ( $\mu\text{m}$ )	-0.719	0.719	0	Strong
2	Mean of shorter side of bounding rectangle ( $\mu\text{m}$ )	-0.714	0.714	0	Strong
3	SD of diagonal length ( $\mu\text{m}$ )	-0.679	0.679	0	Strong
4	SD of shorter side of bounding rectangle ( $\mu\text{m}$ )	-0.677	0.677	0	Strong
5	SD of deviation from mode angle ( $^{\circ}$ )	-0.592	0.592	0	Strong
6	Mean of area ( $\mu\text{m}^2$ )	-0.587	0.587	0	Strong
7	SD of tilt angle ( $^{\circ}$ )	-0.580	0.580	0	Strong
8	Mean of number of detected cuticles	0.579	0.579	0	Moderate
9	SD of area ( $\mu\text{m}^2$ )	-0.578	0.578	0	Moderate
10	Mean of equivalent diameter ( $\mu\text{m}$ )	-0.570	0.570	0	Moderate
11	Mean of aspect ratio	0.568	0.568	0	Moderate
12	SD of aspect ratio	0.512	0.512	0	Moderate
13	SD of equivalent diameter ( $\mu\text{m}$ )	-0.500	0.500	0	Moderate
14	Mean pixel value – Grayscale	-0.402	0.402	0	Moderate
15	Mean of roundness	0.294	0.294	0	Weak
16	Mean of maximum absolute length ( $\mu\text{m}$ )	-0.268	0.268	0	Weak
17	SD of longer side of bounding rectangle ( $\mu\text{m}$ )	0.196	0.196	0.004	Weak
18	Mean of longer side of bounding rectangle ( $\mu\text{m}$ )	-0.161	0.161	0.014	Weak
19	Mean of hair width ( $\mu\text{m}$ )	0.159	0.159	0.011	Weak
20	SD of roundness	-0.158	0.158	0.015	Weak
21	SD of maximum absolute length ( $\mu\text{m}$ )	0.150	0.150	0.03	Weak
22	Mean of tilt angle ( $^{\circ}$ )	-0.040	0.040	0.562	-
23	Mean of deviation from mode angle ( $^{\circ}$ )	0.010	0.010	0.861	-

Notes:

- Pearson's r: Correlation coefficient between the feature and the target, r: Absolute value of Pearson's r, p-value: Statistical significance of the correlation, SD: Standard Deviation,  $\mu\text{m}$ : Micrometer

Correlation Groups:

- Strong: (  $p < 0.05$  ) and absolute value of correlation coefficient  $\geq 0.580$ , Moderate: (  $p < 0.05$  ) and absolute value  $\geq 0.400$  but  $< 0.580$ , Weak: (  $p < 0.05$  ) and absolute value  $< 0.400$ , None (-): Does not meet the above criteria.

**Table 3.** Impact of Correlation-Based Feature Selection on Model Predictive Performance

Correlation Group	Number of Selected Features	Total Combinations	Combinations Outperforming Baseline	Percentage (%)	Judgment
<b>Strong</b>	1	7	4	57.1	Neutral
	2	21	21	<b>100.0</b>	Good
	3	35	35	<b>100.0</b>	Good
	4	35	35	<b>100.0</b>	Good
	5	21	21	<b>100.0</b>	Good
<b>Moderate</b>	1	7	1	14.3	Poor
	2	21	17	81.0	Neutral
	3	35	33	94.3	Neutral
	4	35	35	<b>100.0</b>	Good
	5	21	21	<b>100.0</b>	Good
<b>Weak</b>	1	7	0	0.0	Poor
	2	21	6	28.6	Poor
	3	35	19	54.3	Neutral
	4	35	28	80.0	Neutral
	5	21	21	<b>100.0</b>	Good

Judgment Criteria:

- Good: All combinations of selected features within the correlation group outperformed the baseline model (i.e., achieved lower RMSE).

- Neutral: More than half of the combinations outperformed the baseline.

- Poor: Less than half of the combinations outperformed the baseline.

error between predicted and actual values, and a smaller RMSE reflects better model accuracy.  $R^2$  was also calculated to assess how well the models explained the data variance, with values closer to 1 indicating higher prediction accuracy.

Table 3 presents the total number of models created for each correlation group, as well as the number of models that outperformed the baseline (i.e., having a smaller RMSE). In the strong correlation group, selecting one feature showed that 4 out of 7 models outperformed the baseline.

### 3.3. Validation of the Estimation Results Using the Cuticle Layer Count Estimation Model

To validate the effectiveness of the developed model for estimating the overlapping cuticle layer counts, predictions were made using features extracted from classified hair surface images. Validation was conducted using 82,159 models constructed by randomly selecting one to six features from the 21 features that showed significant correlations with the overlapping cuticle layer counts, as shown in Table 2. The coefficient of determination ( $R^2$ ) and root mean square error (RMSE) were calculated as performance metrics.

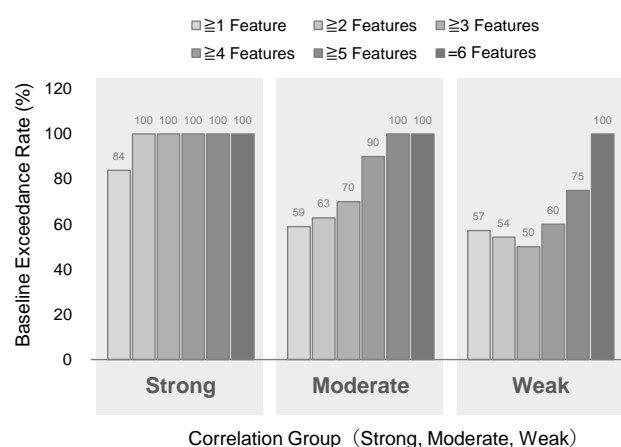


**Figure 3.** Baseline Exceedance Rates According to the Number of Selected Features Across Correlation Groups

Baseline exceedance rates based on the number of selected explanatory features (1–6) from groups categorized by correlation strength (strong, moderate, weak).

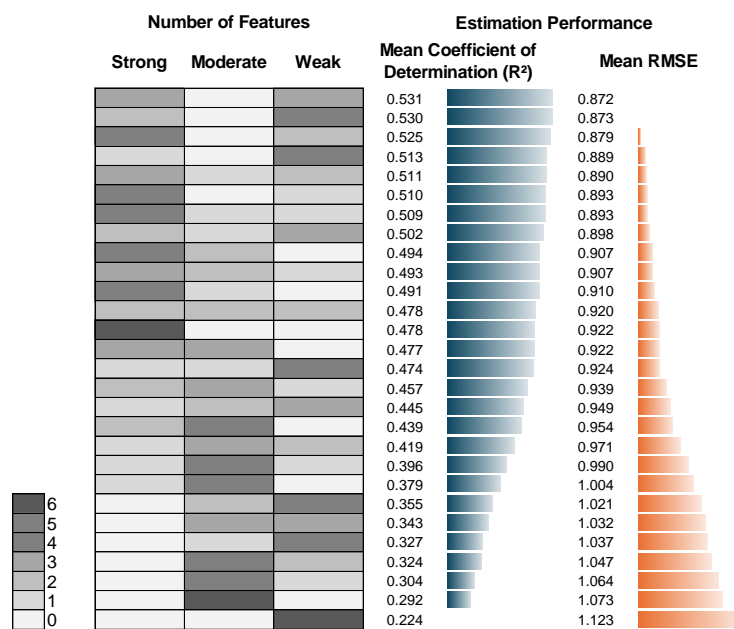


**Figure 4.** Relationship Between Feature Selection Composition (Six Features) and Model Performance Metrics

Visualization of model performance metrics based on feature selection patterns involving six selected features from groups categorized by correlation group (strong, moderate, weak). The heatmap represents the number of features selected from each group, with darker shades indicating higher counts. The bar graphs show the mean coefficient of determination ( $R^2$ ) in blue and the mean root mean square error (RMSE) in red. Baseline exceedance rates were also evaluated across different feature selection compositions.

The relationship between the number of selected features from the 21 features and the estimation performance was evaluated. In the strong correlation group, selecting two or more features resulted in all models exceeding the baseline performance. In the moderate correlation group, models with four or more selected features, and in the weak correlation group, models with five or more selected features, exceeded the baseline in more than 75% of cases (Fig. 3).

Furthermore, under the condition where six features were selected, the models were categorized based on the number of features selected from each correlation group, and the mean  $R^2$  and RMSE values were compared across the groups. Although selecting more features from the strong correlation group tended to improve estimation accuracy, models composed solely of strongly correlated features did not always achieve the highest accuracy. Rather, combining features from the moderate and weak correlation groups appropriately resulted in even better prediction performance (Fig. 4). This trend was also observed when selecting four or five features.

Finally, a representative high-performing model was selected, and a scatter plot of the actual versus predicted overlapping cuticle layer counts was created (Fig. 5). The results demonstrated that high estimation accuracy could be achieved through appropriate feature selection.

#### 4. Discussion

In recent years, AI-based skin diagnosis services using facial images have become widespread, facilitating the optimization of skincare based on individual skin conditions and characteristics. However, AI diagnostic technologies specific to hair care have not yet been fully established due to challenges in hair imaging and analysis methods. This study developed an AI model that accurately estimates the overlapping cuticle layer counts from hair surface images, aiming to provide personalized hair treatments based on hair damage and characteristics.

The AI model developed in this study utilized several morphological features of the cuticle surface (the mean and standard deviation of diagonal length, shorter side of bounding rectangle, tilt angle, area, and deviation from mode angle) as explanatory features, resulting in highly accurate estimations. This supports the findings of Zhang et al. [12], who demonstrated that quantitative surface features are effective for damage assessment in hair.

The machine learning results confirm that in hair surface images, when the cuticle direction is aligned, more cuticle regions are recognized, and features such as shorter lengths of the diagonal width and shorter side of bounding rectangle, along with a smaller area, are associated with less cuticle damage (Table 2). Furthermore, the relationship between the number of

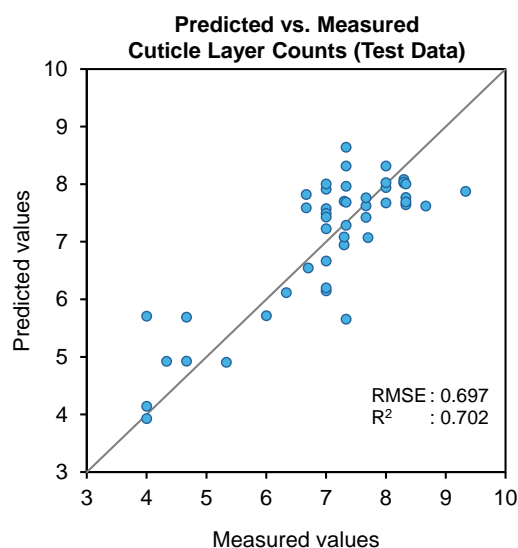


**Figure 5.** Prediction Accuracy of Cuticle Layer Count Estimation Model on Test Data

A scatter plot comparing the predicted and measured overlapping cuticle layer counts using a high-accuracy model on the test dataset. The results demonstrate that appropriate feature selection enables accurate estimation, with a root mean square error (RMSE) of 0.697 and a coefficient of determination ( $R^2$ ) of 0.702.

selected features and estimation performance was investigated by classifying the features by correlation strength. When selecting two or more features from the strong correlation group, all models outperformed the baseline (Figure 3). In contrast, models with four or more features selected from the moderate correlation group, and five or more from the weak correlation group, exceeded the baseline in over 75% of cases, suggesting that selecting features with higher correlations improves model performance.

Moreover, when selecting six features, it was found that models consisting solely of strong correlation features did not always achieve the highest accuracy. Instead, combining features from the moderate and weak correlation groups improved estimation accuracy (Figure 4). This suggests that, for hair characteristics estimation, using independent variables with low multicollinearity is crucial.

It is generally accepted that the overlapping cuticle layer counts in Japanese hair is between 6 and 10. When the cuticle undergoes physical or chemical damage, gradual peeling occurs, resulting in increased exposure and changes in surface morphology, as demonstrated in previous studies [13].

In this study, features such as cuticle area and tilt angle showed a strong correlation with the overlapping cuticle layer counts, reflecting structural changes associated with damage. Specifically, as cuticle peeling progresses randomly rather than in a single direction, the shape becomes irregular, and there is an increasing variability in the tilt angle. Additionally, it has been reported that there are racial differences in the overlapping cuticle layer counts and peeling shapes [7]. Therefore, when applying this AI model to other populations, the structural meanings and contributions of the features correlating with cuticle overlaps may differ, requiring further validation with more diverse hair samples.

The overlapping cuticle layer counts is a key factor in determining hair characteristics and could serve as a valuable indicator for stylists when deciding on treatment methods. The AI model developed in this study can objectively estimate the overlapping cuticle layer counts, making it a useful tool for stylists in treatment decision-making. This could facilitate easier selection of chemicals and treatment times for perm and color treatments, helping to prevent treatment-related issues. Moreover, by conducting detailed data analysis, including factors such as gender and age, estimation accuracy can be improved, making it possible to predict individual hair characteristics in the future, thus contributing to the creation of novel aesthetic value throughout life.

## 5. Conclusion

In this study, we developed an AI-based estimation model capable of accurately predicting the overlapping cuticle layer counts using multiple morphological features extracted from hair surface images. The proposed model provides a valuable quantitative indicator of hair health and has demonstrated strong potential for enhancing the quality of cosmetic hair treatments.

Future work will focus on expanding the dataset to include a broader range of attributes, such as ethnicity, gender, and age, and on analyzing temporal changes in hair characteristics. These advancements are expected to further improve the model's predictive capabilities, enabling the development of personalized hair care recommendations. Ultimately, this will facilitate the practical application of AI in the beauty industry and contribute to the delivery of optimized aesthetic value tailored to individual needs.

## Reference

- [1] Nagase, S., Kajiura, Y., Mamada, A., Abe, H., Shibuichi, S., Satoh, N., Itou, T., Shinohara, Y., & Amemiya, Y. (2009). Changes in structure and geometric properties of human hair by aging. *Journal of Cosmetic Science*, 60(6), 637-648.
- [2] Kim, Y. D., Jeon, S. Y., Ji, J. H., & Lee, W. S. (2010). Development of a classification system for extrinsic hair damage: Standard grading of electron microscopic findings of damaged hairs. *American Journal of Dermatopathology*, 32(5), 432-438. <https://doi.org/10.1097/DAD.0b013e3181c38549>
- [3] Lee, S. Y., Choi, A. R., Baek, J. H., Kim, H. O., Shin, M. K., & Koh, J. S. (2016). Twelve-point scale grading system of scanning electron microscopic examination to investigate subtle changes in damaged hair surface. *Skin Research and Technology*, 22(4), 406-411. <https://doi.org/10.1111/srt.12279>
- [4] Sato, S., Sasaki, Y., Adachi, A., & Omi, T. (2013). Reduction and block staining of human hair shafts and insect cuticles by ammonium thioglycolate to enhance transmission electron microscopic observations. *Journal of Cosmetics, Dermatological Sciences and Applications*, 3(2), 157-161. <https://doi.org/10.4236/jcdsa.2013.32025>
- [5] Gurden, S. P., Monteiro, V. F., Longo, E., & Ferreira, M. M. C. (2004). Quantitative analysis and classification of AFM images of human hair. *Journal of Microscopy*, 215(1), 13-23. <https://doi.org/10.1111/j.0022-2720.2004.01350.x>
- [6] Swift, J. A., & Smith, J. R. (2000). Atomic force microscopy of human hair. *Scanning*, 22(5), 310-318. <https://doi.org/10.1002/sca.4950220506>
- [7] Takahashi, T., Hayashi, R., Okamoto, M., & Inoue, S. (2006). Morphology and properties of Asian and Caucasian hair. *Journal of Cosmetic Science*, 57(4), 327-338.
- [8] Lagarde, J. M., Peyre, P., Redoules, D., Black, D., Briot, M., & Gall, Y. (1994). Confocal microscopy of hair. *Cell Biology and Toxicology*, 10(5-6), 301-304. <https://doi.org/10.1007/BF00755774>
- [9] He, K., Zhang, X., Ren, S., & Sun, J. (2016). Deep residual learning for image recognition. In Proceedings of the 2016 Conference on Computer Vision and Pattern Recognition (pp. 770–778). IEEE.
- [10] Szegedy, C., Vanhoucke, V., Ioffe, S., Shlens, J., & Wojna, Z. (2016). Rethinking the inception architecture for computer vision. In Proceedings of the 2016 Conference on Computer Vision and Pattern Recognition (pp. 2818–2826). IEEE.
- [11] Dosovitskiy, A., Beyer, L., Kolesnikov, A., Weissenborn, D., Zhai, X., Unterthiner, T., Dehghani, M., Minderer, M., Heigold, G., Gelly, S., Uszkoreit, J., & Houlsby, N. (2021). An image is worth 16x16 words: Transformers for image recognition at scale. In Proceedings of the 2021 International Conference on Learning Representations (pp. 1–22). Open-Review.
- [12] Zhang, L., Man, Q., & Cho, Y. I. (2021). Deep-learning-based hair damage diagnosis method applying scanning electron microscopy images. *Diagnostics*, 11(10), 1831. <https://doi.org/10.3390/diagnostics11101831>
- [13] Lee, M. S., & Chang, B. S. (2019). Morphological damage procedures of hair surface treated with repetitive oxidation coloring agent. *Medico Legal Update*, 19(2), 533–539.